

Fast, flexible alternatives to regular grid designs for spatial capture-recapture

Ian Durbach^{*1,2}, David Borchers¹, Chris Sutherland^{1,3}, and Koustubh Sharma⁴

¹Centre for Research into Ecological and Environmental Modelling, University of St Andrews, UK

²Centre for Statistics in Ecology, the Environment, and Conservation, University of Cape Town, South Africa

³Department of Environmental Conservation, University of Massachusetts-Amherst, USA

⁴Snow Leopard Trust, USA

Abstract

1. Spatial capture-recapture (SCR) methods use the location of detectors (camera traps, hair snares, live-capture traps) and the locations at which animals were detected (their spatial capture histories) to estimate animal density. Despite the often large expense and effort involved in placing detectors in a landscape, there has been relatively little work on how detectors should be located. A natural criterion is to place traps so as to maximize the precision of density estimators, but the lack of a closed-form expression for precision has made optimizing this criterion computationally demanding.
2. Recent results by Efford and Boulanger (2019) show that precision can be well approximated by a function of the expected number of detected individuals and expected number of recapture events, both of which can be evaluated at low computational cost. We use these results to develop a method for obtaining survey designs that optimize this approximate precision for SCR studies using count or binary proximity detectors, or multi-catch traps.
3. We show how the basic design protocol can be extended to incorporate spatially-varying distributions of activity centres and animal detectability. We illustrate our approach by simulating from a camera trap study of snow leopards in Mongolia and comparing estimates from our designs to those generated by regular or optimized grid designs. Optimizing detector placement increased the number of detected individuals and recaptures, but this did not always lead to more precise density estimators due of less precise estimation of the effective sampling area. In most cases the precision of density estimators was comparable to that obtained with grid designs, with improvement in some scenarios where approximate $CV(\hat{D}) < 20\%$ and density varied spatially.
4. Designs generated using our approach are transparent and statistically grounded. They can be produced for survey regions of any shape, adapt to known information about animal density and detectability, and are potentially easier and less costly to implement. We recommend their use as good, flexible candidate designs for SCR surveys when reasonable knowledge of model parameters exists. We provide software for researchers to construct their own designs, in the form of updates to design functions in the R package *oSCR*.

*Corresponding author: id52@st-andrews.ac.uk

This article has been accepted for publication and undergone full peer review but has not been through the copyediting, typesetting, pagination and proofreading process, which may lead to differences between this version and the [Version of Record](#). Please cite this article as [doi: 10.1111/2041-210X.13517](https://doi.org/10.1111/2041-210X.13517)

39 1 Introduction

40 Spatial capture-recapture (SCR) models are commonly used to estimate animal abundance and
distribution from surveys that use detectors at fixed locations to record the presence of marked
42 animals at those locations, in the form of spatial capture histories (Borchers & Efford, 2008;
Royle, Chandler, Sollmann, & Gardner, 2014). Detection data can be collected by camera
traps, hair snares and scat surveys, live-capture traps, area searches, or acoustic detectors,
with presence recorded accordingly as an image, DNA sample, animal, or audio recording.
46 SCR methods jointly estimate the parameters of a spatial model quantifying expected animal
47 activity centre density at all points in the survey region, and a detection model that quantifies
48 the probabilities of detection, given the activity centre locations and the detector locations.

49 All SCR surveys have to decide where to place detectors to best address survey objectives.
50 For wildlife surveys, the focus is often animal density or abundance, and survey designs ideally
51 minimize the mean square error of density (or abundance) estimators, equal to the square of the
52 bias plus the variance. SCR estimators have been shown to be unbiased under a wide range of
detector arrangements (Efford, 2019a; Efford & Boulanger, 2019; Sun, Fuller, & Royle, 2014), so
54 that designs that maximize the precision of density (or abundance) estimators – or equivalently,
55 minimize the coefficient of variation of the density estimator $CV(\hat{D})$ – could reasonably be
considered optimal (Efford & Boulanger, 2019; Royle et al., 2014).

57 The SCR survey design goal we consider here is to choose the locations of a fixed number
58 of detectors in a survey region so as to minimize $CV(\hat{D})$, without any further constraints on
59 detector locations (for example, that these must lie on a regular grid). There is currently no
60 method for doing this, which is surprising given the monetary cost and effort involved in setting
up an SCR survey. The reason is that until recently the only way to calculate variance (as
well as bias) with a given design was by computationally demanding simulation, requiring that
63 an SCR model be fit to each of a large enough number of simulated datasets to achieve stable
64 estimates. This allows small numbers of candidate designs to be compared (Clark, 2019; Efford,

65 2019b; Kristensen & Kovach, 2018; Sollmann, Gardner, & Belant, 2012; Sun et al., 2014), but
66 optimizing detector locations requires potentially thousands of evaluations, and this has been
67 computationally prohibitive. As a result, decisions about how to modify candidate designs and
68 when to stop the design process have been left to subjective judgement. Exceptions are Royle et
69 al. (2014) and Dupont, Royle, Nawaz, and Sutherland (2020), who considered designs optimizing
70 a suite of objective functions, which are either related only indirectly to the main objective of
71 estimating animal density precisely by focusing on detection parameters, or relied on simplifying
72 assumptions that are untested and available only for certain types of detection models.

73 As a result, most SCR surveys use some combination of broad guidelines on detector spacing
74 and layout to generate a small set of candidate designs, possibly followed by a simulation-based
75 comparison of these candidate designs on statistical criteria such as relative bias and precision.
76 Being general, guidelines typically recommend highly regular designs that arrange detectors
in a regularly-spaced grid, or else in clusters, with the spacing between detectors chosen so
that individual animals have a reasonable chance of being detected at more than one detector
79 (Clark, 2019; Efford & Fewster, 2013). The motivation for using these designs is that they can be
80 expected to return unbiased density estimates with relatively good precision under a wide range
81 of conditions (Efford & Fewster, 2013). However, placing detectors at regular intervals may be
82 impossible in some survey areas, and better designs may be achievable without the constraint
83 of regular spacing even if that spacing is feasible (Dupont et al., 2020).

The only way to compute bias in SCR-based density estimates remains by computationally
85 intensive simulation, but a recent approximation of $CV(\hat{D})$ (Efford & Boulanger, 2019) pro-
86 vides a sensible, computationally feasible design criterion for optimizing detector locations with
87 unbiased estimators. Their approximation is

$$CV(\hat{D}) \approx 1/\sqrt{\min\{E(n), E(r)\}} \quad (1)$$

88 where both the expected number of first captures $E(n)$ and recaptures $E(r)$ can be evaluated
89 quickly using numerical integration over a habitat mask of the survey region. Two main uses for

90 the approximation are suggested: fast comparison of candidate designs, and optimizing detector
91 spacing for a regular grid of detectors by numerically finding the spacing for which $E(n) = E(r)$.
92 In this paper we show how this approximation can be combined with optimization methods to
93 determine detector locations that maximize the approximate precision of density estimates,
94 without constraint to a regular layout. The resulting detector locations reflect the best available
95 balance between a wide spacing that results in few recaptures but detects many individuals, and
96 clustering detectors close together so that an animal seen on one detector will likely be seen at
97 others (Royle et al., 2014; Sollmann et al., 2012). We call these $\min(n, r)$ designs.

98 Calculations of $E(n)$ and $E(r)$ remain fast even if their inputs vary spatially, for example as
99 a function of covariates. Our design procedure can thus be extended to provide designs for any
100 extension to the basic SCR model that permits fast evaluation of $E(n)$ and $E(r)$. We illustrate
101 this by developing designs incorporating non-uniform animal density and spatially-varying de-
102 tection covariates. We show that the accuracy of the $CV(\hat{D})$ approximation remains good when
103 density varies spatially, extending the results of previous simulations assuming constant den-
104 sity (Efford & Boulanger, 2019), and supporting the use of the approximation in this extended
105 context.

106 Using the $CV(\hat{D})$ approximation as a design criterion relies heavily on the accuracy of the
107 approximation not depending on detector configuration, except through the expected number
108 of first captures and recaptures. We show that although designs that maximize approximate
109 precision lead to greater sample sizes than regular grid designs, these gains are often offset by
110 lower precision in other estimators, most notably those related to the effective area surveyed,
111 which are not accounted for in the approximation. Nevertheless, $\min(n, r)$ designs are com-
112 petitive with regular grid designs in most cases and sometimes outperform them, particularly
113 when animal activity centre density varies spatially. They have the benefit of flexibility, being
114 applicable to study regions of any shape, and can be expected to be easier and less costly to
115 implement, owing to detectors being more clustered.

116 We illustrate the application of our proposed approach by revisiting a camera trap survey
117 of snow leopards in the Tost Mountains of Mongolia. Using an existing survey provides a
118 background context and plausible ranges for model parameters, and allows for comparison with
119 actual design practices, all of which are useful for illustration and interpretability.

120 **2 Materials and Methods**

121 **2.1 Components of the SCR model**

122 Spatial capture-recapture (SCR) models comprise a spatial model of the population and a spatial
123 model of the detection process. These are fitted jointly to the capture histories of detected
124 individuals to provide estimates of, among other quantities, the density of individuals within
125 an area, the effective area surveyed, and population size (Borchers & Efford, 2008; Royle et al.,
126 2014).

127 The spatial model of the population describes the distribution of activity centres in the
128 landscape, each animal represented by its activity centre. Locations of animal activity centres
129 are assumed to be generated by a Poisson process with density (“intensity”) $D(\mathbf{x})$ at a point
130 \mathbf{x} on a habitat mask A representing the survey region. The mask (or state space) is a two-
131 dimensional polygon large enough that animals living outside the mask have a negligible chance
132 of being detected, often obtained by adding a buffer region around detector locations. Density
133 may be constant over space, corresponding to a random uniform distribution of animals in
134 space, or may vary as a function of spatially-varying covariates. The number N of activity
135 centres in A can either be treated as a Poisson random variable, in which case the number
136 of activity centres N and their locations follows a Poisson point process, or as a single, fixed
137 realization of that variable, in which case the activity centre locations follow a binomial point
138 process. The approximation in (1) assumes a Poisson point process; for a binomial point process
139 $CV(\hat{D}) \approx \sqrt{1/\min\{E(n), E(r)\} - 1/(DA)}$ (Efford & Boulanger, 2019). In what follows we
140 assume a Poisson point process, but our approach is also applicable to the binomial case.

141 The detection process assumes a survey in which K detectors are placed in a region containing

142 animals, each of which possesses an activity centre, for S survey occasions. The expected
143 number of encounters of an individual whose activity centre is \mathbf{x} at a particular detector k
144 in occasion s is a decreasing function of the distance between the detector and the activity
145 centre, $d_k(\mathbf{x})$. Various functional forms are assumed for this relationship, commonly a half-
146 normal $\lambda(d_k(\mathbf{x})) = \lambda_0 \exp[-d_k(\mathbf{x})/(2\sigma^2)]$, where λ_0 is the cumulative encounter hazard for a
147 detector at the centre of an animal's home range and σ is a scale parameter determining how
148 quickly the encounter rate decreases with distance between detector and activity centre. Both
149 parameters may also vary as a function of spatially-varying covariates measured at detector
150 locations, although a more natural way to make σ depend on spatial covariates is almost always
151 to model conductance of (or resistance to) movement as a function of spatial covariates, as in
152 Sutherland, Fuller, and Royle (2015). The expected number of encounters over all detectors for
153 an animal whose activity centre is \mathbf{x} in occasion s is $\Lambda_s(\mathbf{x}) = \sum_k \lambda(d_k(\mathbf{x}))$ and over all occasions
 $\Lambda(\mathbf{x}) = \sum_s \Lambda_s(\mathbf{x})$. The effective sampling area covered by a survey is $a = \int_{\mathbf{x}} p(\mathbf{x}) d\mathbf{x}$, where
 $p(\mathbf{x})$ is the probability that an animal with an activity centre at \mathbf{x} is detected at least once
156 during the survey. Conceptually, the effective sampling area downweights the area contribution
157 of regions of the habitat mask where the detection probabilities $p(\mathbf{x})$ are low.

158 Encounter data are collected as capture histories recording the presence of individual animals
159 at detectors in each survey occasion. The exact format of the capture histories depends on the
160 kind of detectors used. We use the same three used by Efford and Boulanger (2019), all of
161 which assume that a detector can detect multiple animals at each occasion. Then, animals can
162 be detected (a) at most once across all detectors in each occasion (“multi-catch traps”); (b) at
163 most once at each detector in each occasion (“binary proximity detectors”); or (c) any number
164 of times at each detector in each occasion (“count proximity detectors”).

165 2.2 Design objectives

166 Royle et al. (2014) considered four design objectives – minimizing the trace of the variance-
167 covariance matrix of the MLEs of detection model parameters; minimizing $\text{var}(\hat{p})$, the variance

168 of the MLE of the mean detection probability (the probability that an animal in A is detected
 169 by the survey); maximizing the mean detection probability; and minimizing $\text{var}(\hat{N}_c)$, where
 170 $\hat{N}_c = n/\hat{p}$ is a conditional estimator of N and n is the number of animals detected – while
 171 Dupont et al. (2020) maximized \bar{p}_m , the mean probability that an animal is detected on two or
 172 more detectors. All except the fourth criterion in Royle et al. (2014) relate only indirectly to
 173 obtaining precise estimates of animal density or abundance. The fourth is an appealing design
 174 objective but cannot be calculated in closed form. Royle et al. (2014) provide an approximation,
 175 but this involves calculating all three of the other criteria as inputs, relies on asymptotic variance
 176 calculations that are only valid for Gaussian hazard detection models with Bernoulli observa-
 177 tions, and approximates the variance-covariance matrix of the detection model parameter MLEs
 178 with the inverse of the expected Fisher information matrix under a standard Poisson GLM with
 179 fixed N .

Efford and Boulanger (2019) provide the much simpler approximation in (1), with expected
 numbers of first captures $E(n)$ and recaptures $E(r)$ given by

$$E(n) = \int_{\mathbf{x}} [1 - \exp(-\Lambda(\mathbf{x}))] D(\mathbf{x}) d\mathbf{x} \quad (\text{all detectors}) \quad (2)$$

and

$$E(r) = \int_{\mathbf{x}} \Lambda(\mathbf{x}) D(\mathbf{x}) d\mathbf{x} - E(n) \quad (\text{count proximity detectors}) \quad (3)$$

$$E(r) = \int_{\mathbf{x}} \sum_{s=1}^S \sum_{k=1}^K [1 - \exp\{-\lambda(d_k(\mathbf{x}))\}] D(\mathbf{x}) d\mathbf{x} - E(n) \quad (\text{binary proximity detectors}) \quad (4)$$

$$E(r) = \int_{\mathbf{x}} \sum_{s=1}^S [1 - \exp(-\Lambda_s(\mathbf{x}))] D(\mathbf{x}) d\mathbf{x} - E(n) \quad (\text{multi-catch traps}) \quad (5)$$

182 Our approach can be applied to all three detector types, but for brevity we focus on count
 proximity detectors (eq. (3)) in the remainder of the paper. The approximation has no formal
 183 derivation but relies on two intuitions. The first is that natural variation in animal abundance
 184 sets an effective lower bound on how small $CV(\hat{D})$ can be, so that if the number of animals
 185 is assumed to be Poisson distributed with parameter n , as is commonly done, then this lower
 186

187 bound equals $1/\sqrt{n}$. The second is that recaptures decrease variance in \hat{D} . An exact relationship
188 holds for a simple two-stage mark-recapture study. In that case, population size is estimated
189 with the Lincoln-Petersen estimator $\hat{N} = n_1/(r/n_2)$ where n_1 and n_2 are number of captures
190 at each visit and r is number of recaptured animals that were marked. The variance of this
191 estimator is approximated by $1/r$ (Seber et al., 1982).

192 Simulations reported in Efford and Boulanger (2019) show that values of $CV(\hat{D})$ obtained by
193 approximation closely matched those obtained by simulation across a number of problem settings
194 assuming square arrays and uniform density of activity centres. For some detector geometries,
195 the approximation underestimated $CV(\hat{D})$, in the case of linear detector arrays by 25%. Efford
196 and Boulanger (2019) suggest that in such cases the approximation should be modified by
197 a constant correction factor whose value is determined by simulation. To test whether the
198 approximation also holds for heterogeneous density, we extended the same simulation experiment
199 to include two spatially-varying density surfaces, one in which density was concentrated in the
200 centre of the survey region, and one in which density increased with latitude and longitude, so
201 that the highest densities were in the buffer region of the habitat mask, and assessed the quality
202 of the approximation in these conditions (see Supplementary Material A for further details).

203 **2.3 Optimization**

204 Optimization requires the specification of potential camera locations, a convenient form for
205 which is a grid of points over the survey region, excluding the buffer (Fig. 1a). A small spacing
206 between potential detector locations provides greater flexibility for optimization, but spatial
207 recaptures (detecting the same animal at different detectors) at very small distances provide
208 little information about the shape of the detection function. Adequate spacing is crucial when
209 optimizing any design criterion that treats all spatial recaptures as equivalent (e.g. $\min(n, r)$ and
210 \bar{p}_m designs) because the total number of spatial recaptures is maximized by placing detectors as
211 close together as is allowed by the spacing. This reduces spatial coverage (and thus, n) and leads
212 to many recaptures at relatively uninformative fractions of σ , both of which serve to inflate the

213 CV of the effective sampling area a . Guidelines from simulations with square grids (Efford and
214 Boulanger (2019), also our Fig. 2) cannot be applied directly to the choice of spacing of *possible*
215 detector locations, but suggest a minimum spacing no less than $\sigma/2$. We used a slightly more
216 conservative spacing of $2\sigma/3$.

217 Selecting a design minimizing (1) involves a difficult combinatorial optimization problem for
218 which exact methods are not available. The solution space consists of all $\binom{M}{K}$ possible ways of
219 allocating K detectors across a discretized grid of M possible locations. This is typically an
220 enormous number (with 500 possible locations and 50 cameras, there are 10^{69} possible designs),
221 precluding enumeration; in addition the objective function is non-linear. Various stochastic or
222 approximate solution methods might be used. We initially used a modified Federov algorithm
223 as implemented in Royle et al. (2014), but these tended to produce isolated small clusters of
224 detectors that can be expected to be biased (Clark, 2019) and for which $CV(\hat{D})$ was poorly
225 approximated (Fig. 1c). We then used a standard genetic algorithm implemented in the R
226 package `kofnGA` (Wolters, 2015), following Dupont et al. (2020), that is much less susceptible
227 to this problem (Fig. 1e). The algorithm begins by generating a population of random designs,
228 typically several hundred. These are evaluated using the design criterion, with good designs
229 selected preferentially and with replacement. Selected designs are randomly paired, and each
230 design in a pair exchanges some proportion of its locations with its partner to create two new
231 designs. A final mutation step potentially replaces, with a small probability, each location with
232 a randomly selected one. Over all pairs, these new designs constitute the next population, which
233 again undergoes selection, location exchange, and mutation. The process continues for a fixed
234 number of iterations or until convergence is achieved.

235 As the optimization relies only on expected values of n and r , it has no inbuilt way of avoiding
236 “pathological” designs (Efford & Boulanger, 2019) in which detectors cover too small an area,
237 or are spaced too far apart, for reliable and unbiased estimates of SCR model parameters. To
238 prevent the optimizer straying toward, or selecting, these designs, we added a large penalty term

239 to the objective function in (1), incurred by any designs that do not satisfy some pre-defined
240 desirable criteria. Since these are mainly used to rule out undesirable designs, various criteria are
241 possible (Efford & Boulanger, 2019). We constrained designs to have at least as many detectors
242 separated by $2.5-3.5\sigma$ and $3.5-4.5\sigma$ as a regular 2σ grid, to encourage reliable estimation of σ
243 (Fig. 1).

244 **2.4 Case study: camera trap survey of snow leopards in Tost, Mongolia**

245 The Tost Mountains are a rugged mountain range occupying an area of $\sim 2100\text{km}^2$ and are
246 separated from nearby ranges by several kilometers of steppe that discourage snow leopard
247 movement between ranges, so that in previous analyses the area has been treated as closed.
248 Camera trap surveys have been conducted since 2009 as part of long-term snow leopard moni-
249 toring projects (K. Sharma et al., 2014). Snow leopards have large home ranges of $80-700\text{ km}^2$ in
250 size (Johansson, Simms, & McCarthy, 2016) and this, together with difficult terrain and harsh
251 environments, have historically made assessment challenging and only amenable to camera trap
252 surveys, of which a fairly large number have been carried out (e.g. Alexander, Gopaldaswamy,
253 Shi, & Riordan, 2015; McCarthy et al., 2008; K. Sharma et al., 2014; R. K. Sharma, Bhatnagar,
254 & Mishra, 2015).

255 A camera trap survey of Tost conducted in 2012 (K. Sharma et al., 2014) collected 14
256 first captures and 40 recaptures using an array of 40 camera traps, placed predominantly in
257 areas of rugged terrain (Supplementary Material B). Potential locations for placing cameras
258 were subjectively identified by regional experts based on landscape features suggesting broadly
259 favourable snow leopard habitat. Camera trap locations were identified by surveying 2-5 km
260 on foot in the mountains around each potential location and searching for fresh snow leopard
261 signs (scrapes, urine markings) or, in the absence of such markings, favourable features such as
262 paths along ridgelines, overhanging rocks or steep canyon walls. Emphasis was thus on selecting
263 broad areas, and precise camera locations, where the possibility of capturing snow leopards was
264 high. Cameras were typically tightly spaced, with 25% of cameras being within 2km of another

Figure 1: Illustration of optimizing SCR design; (a) potential detector locations with spacing $\sigma/2$; designs selected by (b) a modified Federov algorithm, (c) a modified Federov algorithm with additional constraints on detector spacing, (d) a genetic algorithm, which returns the same design with or without constraints, (e) a typical grid design with 2σ spacing. Designs (b), (c), and (d) all have $E(n) = E(r) = 62.8$, and thus expected $CV(\hat{D}) = 12.6\%$, but simulated $CV(\hat{D})$'s are 30, 15.8, and 16.5%. The design in (b) suffers from inadequate spacing and cluster size, which inflates $CV(\hat{a})$ (27, 9, and 9% respectively). The modified Fedorov algorithm tends towards these designs unless constrained, while a genetic algorithm does not. A regular grid design gives fewer recaptures ($E(n) = 71$, $E(r) = 48$) and hence has a higher approximate $CV(\hat{D}) = 14.4\%$. Despite this, its simulated $CV(\hat{D}) = 15.8\%$ is at least as good as optimized designs, because of more precise estimates of $CV(\hat{a}) = 8\%$ not accounted for in the approximation.

265 camera and 70% of cameras within 4km. Cameras were left in the field for an average of 105.45
266 (SE=11.81) days and took 7-20 days to set up.

267 We first generated $\min(n, r)$ designs¹ for the survey region under the assumption of constant
268 animal activity centre density across the survey region and setting values for SCR model pa-
269 rameters that allowed us to cover the entire area with a regular grid of 60 detectors spaced 2σ
270 apart, while returning expected sample sizes broadly similar to those observed in the real study
271 (20 individuals detected and 24 recaptures, using actual camera locations). We set the activity
272 centre density at $2/100 \text{ km}^2$, towards the higher end of known snow leopard density estimates.
273 Importantly, detector locations in $\min(n, r)$ designs are unaffected by changes in mean animal
274 density, which simply changes the numbers of first captures and recaptures proportionately. The
275 same configurations of detectors (for example, those reported in Fig. 3) would be obtained for
276 any choice of mean activity centre density, although these may result in very different values
277 of $CV(\hat{D})$. All $\min(n, r)$ designs were generated using the genetic algorithm described in the
278 previous section. We used 50 generations (designs typically converged considerably earlier than
279 this), a population size of 1000 and a mutation rate of 1%.

280 Detection function parameters were set to $\sigma = 3\text{km}$ and encounter rate $\lambda_0 = 1$, again on the
281 basis of ballpark similarity to previous studies and to provide roughly the desired number of first
282 captures and recaptures. A buffer of 3σ was used with a spacing of $2\sigma/3 = 2\text{km}$ between mask
283 points (or, equivalently, the centroids of mask cells). Potential camera locations were specified
284 using a grid of points with the same spacing used in the habitat mask.

285 For this “baseline” case we generated $\min(n, r)$ designs for 20-, 40-, and 60-camera arrays.
286 Cameras were treated as count proximity detectors, except in one set of results where we assessed
287 the effect of detector type. For each design we report and discuss differences in the expected
288 number of first captures $E(n)$, recaptures $E(r)$, approximate CV, and detector locations. We
289 then varied SCR model parameters one at a time, and generated further sets of survey designs.

¹All code and output are available at <https://github.com/iandurbach/optimal-secr-design>.

290 We changed λ_0 and σ to 50%, 150%, and 200% of their baseline values of $\lambda_0 = 1$ and $\sigma = 3$, and
291 changed the buffer from a baseline of 3σ to zero to simulate the treatment of the survey region
292 as closed, as had been assumed in previous analyses.

293 We then generated designs for three extensions to the basic SCR model: one with spatial
294 covariate on density, one with a spatial covariate on detectability, and one with spatial covariates
295 on both density and detectability. Designs for a model with spatially-varying density assumed
296 that expected animal activity density depended on a standardized terrain ruggedness index i.e.
297 $D(\mathbf{x}) = \exp(\alpha_{0D} + \alpha_D R(\mathbf{x}))$, where $R(\mathbf{x})$ is the value of the ruggedness covariate at \mathbf{x} and α_{0D} is
298 chosen so that mean animal density across the study area is the same as in the uniform density
299 case. For this set of designs we jointly varied the size of the array (20, 40, or 60 cameras) and
300 the relationship between density and ruggedness ($\alpha_D \in \{-1, 1, 3\}$), with other parameters held
301 fixed at their baseline values ($\lambda_0 = 1$, $\sigma = 3$, 3σ buffer).

302 Optimal designs for a model with spatially-varying detector covariates assumed that ex-
303 pected encounter rate depended on longitude i.e. $\lambda_0(\mathbf{x}) = \exp(\alpha_{0\lambda_0} + \alpha_{\lambda_0} x_1)$, where x_1 is the
304 longitudinal component of \mathbf{x} . We jointly varied the size of the array (20, 40, or 60 cameras) and
305 the relationship between baseline encounter rate and longitude ($\alpha_{\lambda_0} \in \{-0.75, 0.75, 1.5\}$), with
306 other parameters held fixed at baseline values. Where animal density was uniform we used the
307 baseline value $D = 2/100 \text{ km}^2$; where both density and detectability varied spatially we used
308 $\alpha_D = 1$ and $\alpha_{\lambda_0} \in \{-0.75, 0.75, 1.5\}$.

309 We generated sets of designs using two other approaches, again recording $E(n)$, $E(r)$, ap-
310 proximate and simulated CV, detector locations, and between-detector spacings for each design.
311 The first uses a regular grid of detectors with 2σ spacing between traps. We generated a reg-
312 ular grid of K detectors by creating a grid covering the survey region and choosing a subset of
313 K points – an initial grid point and its $K - 1$ nearest neighbours. The initial grid point was
314 chosen randomly when detection was uniform, at the point of highest density or detectability
315 when either these varied spatially, and at the point of highest density when both varied. This

316 encourages a square grid as far as permitted by the irregular survey area and starting point,
317 and places the array in sensible parts of the survey region.

318 The second approach uses a regular grid with detector spacing chosen to minimize approx-
319 imate $CV(\hat{D})$, using the *optimalSpacing* function in the `secrdesign` package (Efford, 2019b).
320 This calculates $E(n)$ and $E(r)$ at various detector spacings and finds the optimal spacing by
321 linear interpolation. We calculated the optimal spacing for each unoptimized grid generated by
322 the first method, and then generated a new grid of detectors using the same process as before.
323 Where the optimal spacing was too large to place the desired number of cameras in the survey
324 region, it was set to the largest spacing that would allow the cameras to be placed.

325 For each scenario and design, we compared approximate CV to an empirical estimate of
326 $CV(\hat{D})$ obtained from simulation. In each case, we simulated 1000 animal populations and
327 associated capture histories, fitted an appropriate SCR model to each capture history, and
328 calculated the CV of the fitted density estimates. Simulated populations, capture histories, and
329 fitted models included spatially-varying density and detection in those scenarios that made use
330 of them. Models were fitted using the R package `secr` (Efford, 2020).

331 **3 Results**

332 **3.1 Approximation accuracy**

333 The approximation of $CV(\hat{D})$ was slightly less accurate when density varied spatially but re-
334 mained broadly reliable (Fig. 2). Underestimation of $CV(\hat{D})$ occurred with small detector
335 spacing (0.25σ), and this underestimation was more severe for one of two non-uniform den-
336 sity scenarios. With detector spacing of $< 1\sigma$, the approximation remained good so long as
337 approximate $CV(\hat{D}) < 20\%$ when density was uniform, with a stricter condition approximate
338 $CV(\hat{D}) < 15\%$ if density varied spatially. Approximation accuracy was relatively poor for a
339 scenario where density increased with latitude and longitude, because the highest-density areas
340 were part of the buffer region of the habitat mask and not accessible to detectors. Although not
341 practically likely, this demonstrates that the approximation is somewhat sensitive to the density

342 surface when this varies spatially.

343 **3.2 Designs under uniform animal density and habitat use**

In the baseline scenario, with only 20 detectors, recaptures were the limiting factor and so
344 detectors were placed close together (Fig. 3a). As detectors were added spacing between cameras
345 increased to detect more animals, until a spatially well-balanced arrangement broadly resembling
346 a space-filling design was obtained (Fig. 3c).

Restarting the optimization process from different starting points led to different designs
347 that for the most part shared the same aggregate properties (Fig. 3d-f; Supplementary material
348 C). When animal density is assumed uniform, it makes little difference exactly where a camera is
349 located, as long as aggregate properties such as detector spacing are preserved. Visible differences
350 between the two designs were greatest in the 20-detector case, but both designs returned very
351 similar approximate $CV(\hat{D})$'s (Table 1).
352

In reality the Tost survey region is closed due to boundaries of steppe that snow leopards
353 avoid. We therefore simulated a scenario with no buffer region (Fig. 3g-i). Shrinking the buffer
354 to zero pulled traps away from the border and towards the centre of the study area, because
355 detectors at or near the border would include areas of known absence in their detection range
356 and thus be inefficient.
357

Changing the encounter rate intercept parameter λ_0 or the scaling parameter σ had a similar
358 effect (Fig. 3j-l for λ_0 , m-o for σ). Decreasing either of these lowered the frequency of recaptures
359 and so caused detectors to be more concentrated (Fig. 3j,m). Increases had the opposite effect,
360 causing detectors to be more spread out (Fig. 3k and n). Large values of σ resulted in many
361 detectors being placed along the boundary of the survey area, with relatively few detectors in
362 the interior (Fig. 3n,o).
363

Designs for binary proximity detectors and especially multi-catch traps tend to be more
364 clustered together than count proximity detectors, given the same background conditions (Fig.
365 3p-r). This happens because binary proximity detectors treat multiple detections of the same
366

Figure 2: Approximation of precision of $CV(\hat{D})$ (solid lines, circles) compared to simulated precision (dashed lines, triangles) for square grids over a range of detector spacings for (a) uniform density of activity centres, (b) density concentrated in the centre of survey region, decreasing with distance from centre (c) density increasing with latitude and longitude, so that the highest densities are in the buffer of the habitat mask. Experimental setup is as for Efford and Boulanger (2019) except that density varies spatially. See Supplementary Material A for further details and results. Approximation accuracy is less robust when density varies spatially but remains broadly reliable.

Figure 3: Examples of $\min(n, r)$ survey designs for an SCR survey of snow leopards in Tost, Mongolia. All plots assume uniform activity centre density across the survey region. Grid cells are 2×2 km and detectors are indicated in red. “Baseline” conditions refer to setting $\lambda_0 = 1$ and $\sigma = 3$, with a 3σ buffer. These and the number of detectors are independently varied in the sub-plots to demonstrate how optimal designs respond to changes in input parameters.

Scen	CV(\hat{D}) (actual)			CV(\hat{D}) (approx)			CV(\hat{a})		
	Min	Grid	G+O	Min	Grid	G+O	Min	Grid	Gr+O
Effect of varying number of detectors									
(a)	60	61	47	30	33	31	32	25	22
(b)	27	24	24	21	23	22	16	14	11
(c)	20	19	20	17	18	18	11	11	8
Effect of random starts									
(d)	57	50	46	30	33	31	28	23	22
(e)	25	24	24	21	23	22	15	14	12
(f)	20	19	19	17	18	18	12	11	8
Effect of zero buffer									
(g)	58	63	44	30	34	34	29	25	22
(h)	26	25	24	21	23	24	16	13	12
(i)	20	20	20	18	19	20	11	11	8
Effect of varying encounter rate λ_0									
(j)	30	44	28	24	33	26	17	25	13
(k)	16	16	16	14	15	15	8	7	6
(l)	15	14	15	14	14	15	7	5	4
Effect of varying movement parameter σ									
(m)	149	88	49	39	36	36	35	26	20
(n)	13	13	14	12	13	13	7	5	4
(o)	11	12	12	10	11	12	4	4	4
Effect of detector type									
(p)	21	21	22	19	22	21	9	12	8
(q)	20	19	20	18	20	19	11	10	7
(r)	21	19	19	17	18	18	12	10	7

Table 1: Comparing approximations of $CV(\hat{D})$ (col. 4-6) with values obtained by simulation (col. 1-3), for each of the scenarios in Fig. 3. Min = $\min(n, r)$ designs; Grid = regular grid designs with 2σ spacing; G + O = regular grid designs with optimal spacing; see Section 2.4 for details. Approximate and simulated values are close when $CV(\hat{D}) < 20\%$. Optimized $\min(n, r)$ designs provide more first captures and recaptures than grid designs, but can still have lower (simulated) precision because their effective sampling areas are less precisely estimated ($CV(\hat{a})$, col. 7-9).

394 density. As a result, $\min(n, r)$ designs remained better than regular 2σ grids in most scenarios
395 involving spatially-varying density, although again usually only by a small margin. Substantial
396 improvements were achieved in some scenarios where areas of high density and high detectability
397 differed substantially (Fig. 4h,i). These scenarios are not biologically plausible but illustrate
398 some of the potential drawbacks of regular designs in more complex environments.

399 Detectors were more concentrated when covariate relationships were stronger (cf. Fig. 4,
400 b,e,h vs. c,f,i), but the increase was not extreme. The incentive of detecting new individuals
401 encouraged clusters of detectors to form away from high-density or high-detectability areas, once
402 these areas had been exploited. Detector locations spanned the majority of the covariate space,
403 even in quite extreme scenarios (Fig. 5). Good coverage of covariate space is important because
404 unbiased estimates of density depend on covariate relationships being accurately estimated, and
405 this is much more likely if the covariate space has been well sampled.

Covariate coverage is not part of the objective function, and so not something that is un-
der direct control of the optimizer. In our application covariate coverage was better when
408 the density-ruggedness relationship was positive than when it was negative, because cells with
409 high ruggedness were concentrated in one area while cells with low ruggedness were dispersed
410 throughout the survey region. In the latter case, it was possible for clusters to be located so
411 that they were far from one another *and* occupied areas of high density (low ruggedness). When
412 the relationship was positive this was not possible. This means that covariate coverage should
always be assessed, for example using rug plots such as Fig. 5.

Figure 4: Designs for scenarios involving spatially-varying density ($D(\mathbf{x})$) or detectability ($\lambda_0(\mathbf{x})$). Activity centre density depends on terrain ruggedness. Baseline encounter rates depend inversely on longitude (highest in west), with activity centre density either uniform (d-f) or also varying spatially (g-i). Panel labels give covariate coefficients, indicating the direction of the assumed relationship. Grid cell colour indicates terrain ruggedness (a-c, g-i), with lighter colours denoting higher values, or longitude values (d-f). Detectors are placed preferentially where density or detectability is expected to be highest in order to maximize the number of animals detected. However, because recaptures must also be considered, concentration of detectors in high density or detection areas is generally not extreme.

Figure 5: Coverage of spatially-varying density and detectability covariates by $\min(n, r)$ designs. Points plot covariate values at the detector locations in Fig. 4a-f, with the curve showing the functional form of the assumed relationship between density and ruggedness. Coverage is better for positive values of α_D in our case study because the method initially places detectors in high-density patches, before spreading into lower-density patches.

Scen	$CV(\hat{D})$ (actual)			$CV(\hat{D})$ (approx)			$CV(\hat{a})$		
	Min	Grid	G+O	Min	Grid	G+O	Min	Grid	Gr+O
Designs with spatially-varying density									
(a)	25	24	30	19	22	21	12	11	6
(b)	19	20	20	17	19	18	7	8	5
(c)	15	19	15	15	16	15	3	8	4
Designs with spatially-varying detection									
(d)	24	22	25	20	21	24	12	8	3
(e)	23	21	40	21	21	25	11	10	4
(f)	23	22	35	22	23	25	8	9	3
Designs with spatially-varying density and detection									
(g)	18	19	19	16	17	18	7	6	5
(h)	24	36	25	18	32	23	14	21	13
(i)	41	62	54	23	76	52	30	41	36

Table 2: Comparing approximations of $CV(\hat{D})$ (col. 4-6) with values obtained by simulation (col. 1-3), for each of the scenarios in Fig. 4. Min = $\min(n, r)$ designs; Grid = regular grid designs with 2σ spacing; G + O = regular grid designs with optimal spacing; see Section 2.4 for details. In contrast to uniform scenarios, optimized designs have higher (simulated) precision than grid designs in scenarios where their effective sampling areas are estimated with similar precision ($CV(\hat{a})$, col. 7-9).

4 Discussion

The optimization of approximate $CV(\hat{D})$ provides statistically grounded guidance on selecting detector locations for SCR surveys. The way in which designs change in response to changes in survey variables (the number of cameras available) or exogenous variables (encounter rate, animal density, movement, buffer size) represents the best available balance between the competing objectives of maximizing the number of animals detected and maximizing the number of recaptures. Designs generated in this way are transparent and objective. They can be adapted for survey regions of any shape, adapt to known information about animal density, detectability, and movement, and are generally more clustered designs that may be easier and less costly to implement than standard grid designs.

The current approximation of $CV(\hat{D})$ is highly accurate when $CV(\hat{D}) < 15\%$ under both uniform and non-uniform animal density, and remains within a few percent of simulated values so long as $CV(\hat{D}) < 20\%$. However, any discrepancy almost always overestimates precision, and by a slightly larger margin for irregular detector arrays than for regular one. This reduces the

428 gains provided by optimizing $\min\{E(n), E(r)\}$ and in our scenarios involving uniform animal
429 density was often sufficient to reverse it, although differences between optimized and regular
430 grid designs were small in all scenarios except near-pathological ones. The $CV(\hat{D})$ of optimized
431 designs can be worse than that of regular 2σ designs, even if they result in more first captures
432 and recaptures, because the effective sampling area of these designs is generally smaller and less
433 precisely estimated, owing to less precise estimates of detection function parameters, particularly
434 σ , that are not accounted for in the approximation. Other approaches that optimize simple
435 functions of sample size or detection probability are likely to face similar challenges. Further
436 investigation may lead to improvements in the approximation but, until then, $\min(n, r)$ designs
437 should not be considered optimal, but rather good, flexible candidate designs to be compared
438 with other designs using simulation.

439 Other factors known to cause poor approximation accuracy are small detector spacing,
440 “pathological designs” in which detectors cover too small an area, or are spaced too far apart,
441 and linear detector arrays (Efford & Boulanger, 2019). Small detector spacings appear attractive
442 because they provide greater flexibility for optimization and generally offer more recaptures, but
443 spatial recaptures at very small distances provide little information on σ , and this ultimately
444 negatively affects $CV(\hat{D})$. We suggest a minimum spacing no less than $\sigma/2$. Narrower spacing
445 may very occasionally be warranted for species that are nearly impossible to recapture (? , e.g.),
446 although in these cases serious consideration should be given as to whether the data collected
447 will be adequate for the use of SCR. Pathological designs can be removed from consideration
448 by heavily penalizing any designs that do not satisfy some pre-defined criteria. Since these are
449 used only to rule out undesirable designs, various criteria are possible (Efford & Boulanger,
450 2019). For example, we constrained designs to have at least as many detectors separated by
451 $2.5-3.5\sigma$ and $3.5-4.5\sigma$ as a regular 2σ grid. Linearity of detectors can in principle be assessed
452 and corrected for at each step of the optimization process, but currently the only way to do
453 this is with computationally intensive simulation that renders optimization impractical. One

454 possibility is to summarize the linearity of an irregular array in a way that allows the correction
455 factor in Efford and Boulanger (2019) to be inferred in a meaningful and computationally feasi-
456 ble way, but we have not pursued this here. Very few of our designs exhibited signs of linearity.
457 Using simulation to carry out *post hoc* checks of $CV(\hat{D})$, with minor manual adjustments to
458 detector placements to break linear arrangements where necessary (also guided by simulation),
459 is probably sufficient in the majority of cases.

460 The precision of density estimates appears to be robust over a wide range of detector place-
461 ments, so long as problems of pathological designs are avoided. Regular designs return $CV(\hat{D})$'s
462 within a few percent of each other over a wide variety of detector spacings (Efford and Boulanger
463 (2019), Fig. 2) and our designs were in turn almost always within a few percent of these. Reg-
464 ular 2σ designs provide an excellent, robust default design. The primary benefit of $\min(n, r)$
465 designs is that they lead to estimators with comparable precision to the best currently available
466 alternatives, while being applicable to any survey region and with the potential to incorporate
467 information about animal behaviour that may in some cases improve precision. Large improve-
468 ments in precision, however, are probably achievable only by using more detectors or increasing
469 survey duration in the majority of cases. Better choices of detector locations will not be able to
470 remedy fundamental deficiencies in animal density or detection rates.

471 Designs that maximize the precision of density estimators without accounting for the possi-
472 bility of bias run the risk of returning biased estimates of density. If this bias is substantial it
473 may outweigh any gains made by reducing variance. Bias is unlikely to be a problem when activ-
474 ity centres are assumed to be uniformly distributed, as several studies have demonstrated that a
475 variety of SCR surveys are unbiased under these conditions (Efford, 2019a; Efford & Boulanger,
476 2019; Sun et al., 2014). We assessed the bias of each of our designs including spatially-varying
477 density and detection (those in Fig. 4) using simulation (see Supplementary Material D for de-
478 tails), and results indicated that these designs returned estimates of density that exhibited little
479 or no bias. We recommend that designs assuming spatially-varying covariates always include

480 a *post hoc* assessment of the coverage of covariates, as well as *post hoc* assessments of possible
481 bias. If the optimized design does not achieve good coverage, we recommend reverting back
482 to simpler designs with regular spacing, or manually adjusting detector locations to improve
483 covariate coverage, followed by a reassessment of $CV(\hat{D})$. It is also possible to build covariate
484 coverage into the optimization as an objective in its own right, although we have not explored
485 this here.

486 Optimal designs place detectors in locations that exploit particular features of animal den-
487 sity and detectability, represented by parameters like λ_0 , σ , and coefficients for any spatial
488 dependencies. While our approach extends to a number of more advanced SCR variants, these
489 will require reasonable knowledge about the parameters of those models, which may only rarely
490 be available before the survey is conducted. Many SCR surveys are designed with little or no
491 knowledge of what values these parameters might take on, and optimized designs may be ex-
492 pected to perform worse than regular designs if parameter values are poorly chosen. We have
493 not investigated this issue in detail for all parameters, but recalculated the approximate $CV(\hat{D})$
494 of all designs using values of λ_0 , σ , or α_1 up to 50% smaller (or 50% larger) than the values
495 used to generate the designs. The approximate CV of $\min(n, r)$ designs remained better than
496 any other candidate designs for almost all conditions (Supplementary Material E). Still, we rec-
497 ommend that optimized designs for any SCR variant only be used where there is good existing
498 knowledge on the possible values of all the parameters of the model, and that simpler designs be
499 used otherwise. In cases where knowledge extends only to σ , an optimal design is inappropriate
500 and a regular-spaced design should be used.

501 Our designs take no account of the cost, monetary or other, of implementing a particular
502 design, and so may end up choosing a costly design on the basis of a small improvement in
503 approximate precision. However, in our scenarios $\min(n, r)$ designs had smaller average spacing
504 between detectors, were more clustered, and had shorter shortest paths through the detector
505 array (Supplementary Material C), all of which suggest lower cost and easier implementation.

506 Design costs can be incorporated into the optimization process, either by rejecting or penalizing
507 costly designs or by including cost minimization as a second objective, but we leave this to future
508 work.

509 5 Conclusion

510 This paper presents an approach for choosing detector locations in SCR surveys so as to maxi-
511 mize the expected precision of density estimates obtained from the later survey. The approach
512 essentially combines the optimization framework used by Dupont et al. (2020), which employs
513 a genetic algorithm to iterately improve candidate designs, with a new objective function using
514 Efford and Boulanger (2019)'s approximation of the (standardized) precision of density, $CV(\hat{D})$.
515 Our approach can in principle be extended to any variant of SCR for which $E(n)$ and $E(r)$ can
516 be rapidly evaluated. Software for constructing $\min(n, r)$ survey designs has been developed
517 based on a modification of the design function $Enrm$ in the R package `secrdesign`, which pro-
518 vides a fast C implementation of $E(n)$ and $E(r)$ (see Supplementary Material F for details, and
519 Supplementary Material G for a minimal working example). Optimization typically takes no
520 more than a few minutes, even for quite large survey regions.

521 The main benefits provided by $\min(n, r)$ designs are a transparent process that reduces the
522 need for difficult and subjective design decisions, for example around detector spacing and clus-
523 tering, flexibility with respect to survey region, the ability to include environmental covariates
524 affecting density, detectability, and movement. Gains in precision are possible with $\min(n, r)$ de-
525 signs, but these are typically modest and occur where precision is already high ($CV(\hat{D}) < 15\%$).
526 Usually, the precision of optimized and regular grids are within a few percent of one another.
527 There seems relatively little downside to including a $\min(n, r)$ design in the candidate set of
528 designs when planning an SCR survey. Simulation is essential as a means of confirming the
529 $CV(\hat{D})$ of any design before final implementation (Efford & Boulanger, 2019).

530 Optimal designs for SCR surveys have received very little attention, which is surprising given

531 the popularity of SCR and the cost and effort involved in conducting many surveys. Our paper
532 develops optimized designs based on an intuitive and statistically grounded criterion, but also
533 raises a number of questions deserving further attention. These include developing a better un-
534 derstanding of the origins of the approximation; potential improvements to the approximation;
535 more comprehensive comparisons of optimal and other design protocols; sensitivity analyses
536 to misspecification of initial parameter values; designs accounting for individual-level (e.g. sex-
537 specific) detection covariates; inclusion of design costs; and optimization of survey duration as
538 well as location.

539 **Acknowledgements**

540 This work was done to support the Population Assessment of the World's Snow Leopards
541 (PAWS) initiative being coordinated by the Global Snow Leopard and Ecosystem Protection
542 Program (GSLEP) through funding from the Global Environment Facility (Trans-boundary co-
543 operation for snow leopard and ecosystem conservation project ID 5886), made available through
544 United Nations Development Program and International Snow Leopard Trust. ID is supported
545 in part by funding from the National Research Foundation of South Africa (Grant ID 90782,
546 105782). We are grateful to the two anonymous reviewers for their detailed and helpful com-
547 ments, which led to a substantially improved manuscript.

548 **Data Availability**

549 All code and output are available at <https://doi.org/10.5281/zenodo.4074086> (Durbach,
550 Borchers, Sutherland, & Sharma, 2020). This provides a permanent link to the version of the
551 repository <https://github.com/iandurbach/optimal-secr-design> used to generate the re-
552 sults in this paper.

553 **Authors' contributions**

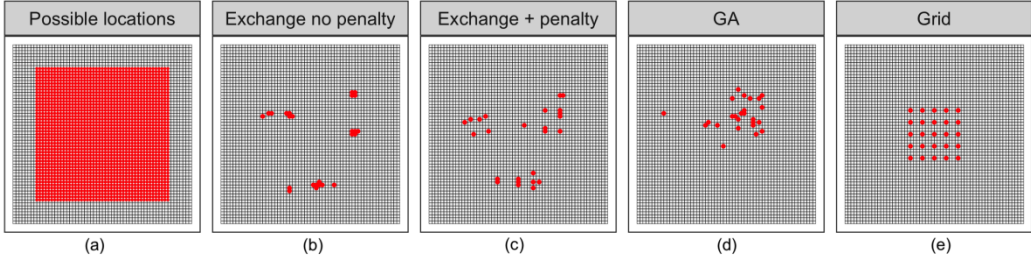
554 All authors conceived the work. DB, ID and CS designed the methodology. KS provided input

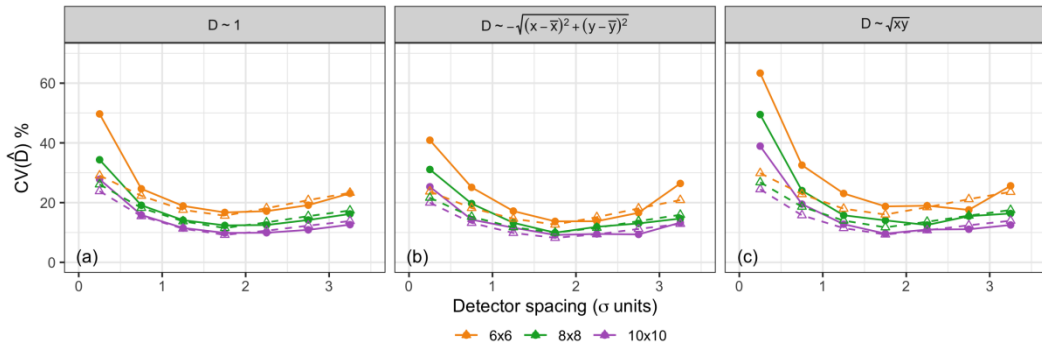
555 on snow leopard survey design, data on existing designs, and feedback on proposed designs. ID
556 performed the simulations and wrote the paper. All authors contributed critically to the drafts
557 and gave final approval for publication.

558 References

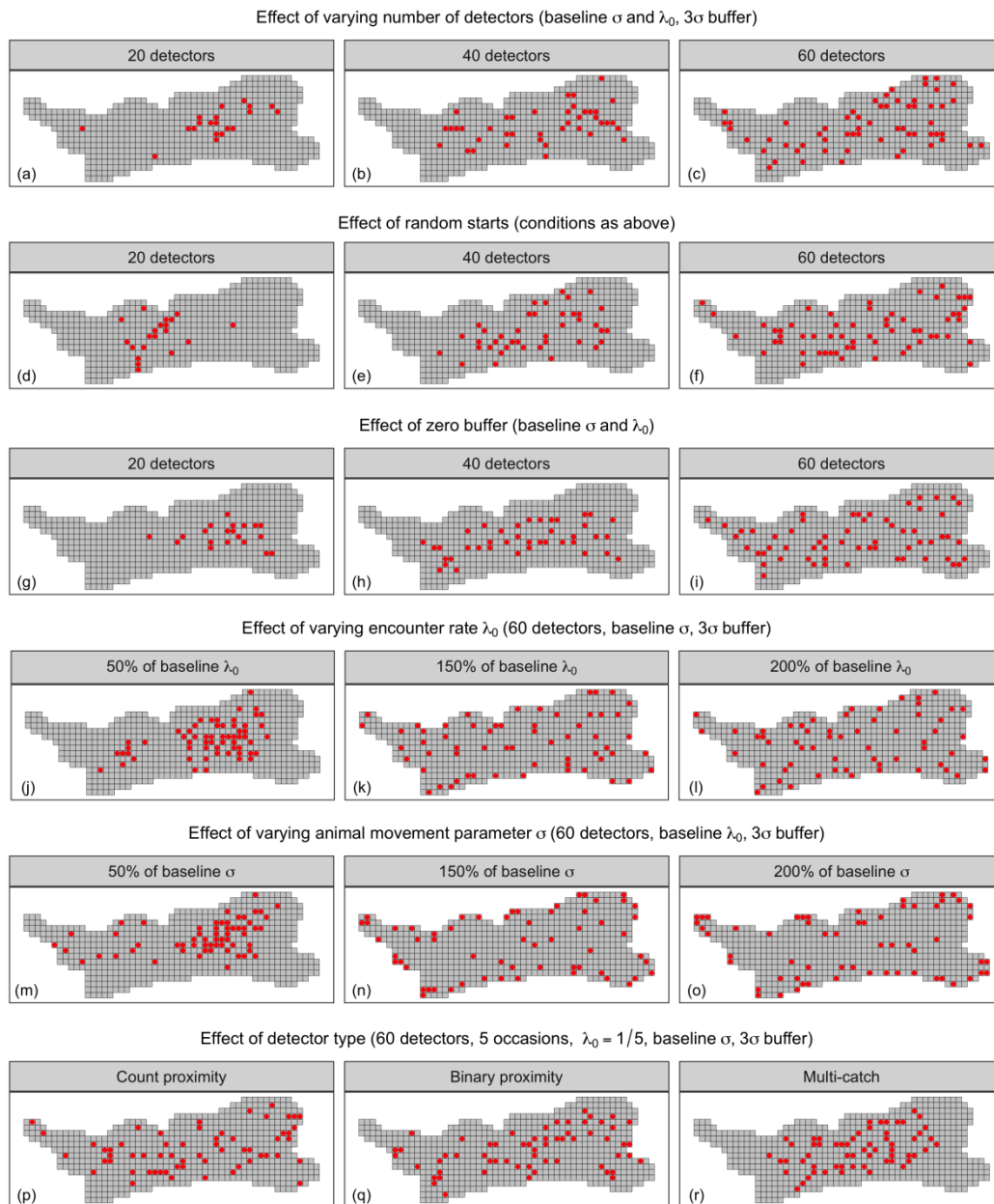
- 559 Alexander, J. S., Gopaldaswamy, A. M., Shi, K., & Riordan, P. (2015). Face value: towards
560 robust estimates of snow leopard densities. *PLoS One*, *10*(8), e0134815.
- 561 Borchers, D. L., & Efford, M. (2008). Spatially explicit maximum likelihood methods for
562 capture–recapture studies. *Biometrics*, *64*(2), 377–385.
- 563 Clark, J. D. (2019). Comparing clustered sampling designs for spatially explicit estimation of
564 population density. *Population Ecology*, *61*(1), 93–101.
- 565 Dupont, G., Royle, J., Nawaz, M. A., & Sutherland, C. (2020). Towards optimal sampling
566 design for spatial capture-recapture. *Ecology*, *In press*.
- 567 Durbach, I., Borchers, D., Sutherland, C., & Sharma, K. (2020). *iandurbach/optimal-secr-*
568 *design: v1.0*. Zenodo. Retrieved from <https://doi.org/10.5281/zenodo.4074086> doi:
569 10.5281/zenodo.4074086
- 570 Efford, M. (2019a). Non-circular home ranges and the estimation of population density. *Ecology*,
571 *100*(2), e02580.
- 572 Efford, M. (2019b). *secrdesign*: Sampling design for spatially explicit capture-recapture
573 [Computer software manual]. Retrieved from [https://CRAN.R-project.org/package=](https://CRAN.R-project.org/package=secrdesign)
574 *secrdesign* (R package version 2.5.7)
- 575 Efford, M. (2020). *secr*: Spatially explicit capture-recapture models [Computer software manual].
576 Retrieved from <https://CRAN.R-project.org/package=secr> (R package version 4.2.2)
- 577 Efford, M., & Boulanger, J. (2019). Fast evaluation of study designs for spatially explicit
578 capture-recapture. *Methods in Ecology and Evolution*, *10*, 1529–1535.
- 579 Efford, M., & Fewster, R. (2013). Estimating population size by spatially explicit capture–
580 recapture. *Oikos*, *122*(6), 918–928.
- 581 Johansson, Ö., Simms, A., & McCarthy, T. (2016). From vhf to satellite gps collars: advance-
582 ments in snow leopard telemetry. In *Snow leopards* (pp. 355–365). Elsevier.
- 583 Kristensen, T. V., & Kovach, A. I. (2018). Spatially explicit abundance estimation of a rare
584 habitat specialist: implications for secr study design. *Ecosphere*, *9*(5), e02217.
- 585 McCarthy, K. P., Fuller, T. K., Ming, M., McCarthy, T. M., Waits, L., & Jumabaev, K. (2008).
586 Assessing estimators of snow leopard abundance. *The Journal of Wildlife Management*,
587 *72*(8), 1826–1833.
- 588 Royle, J. A., Chandler, R. B., Sollmann, R., & Gardner, B. (2014). *Spatial capture-recapture*.
589 Elsevier.
- 590 Seber, G. A. F., et al. (1982). *The estimation of animal abundance and related parameters*
591 (Vol. 8). Blackburn press Caldwell, New Jersey.
- 592 Sharma, K., Bayrakismit, R., Tumursukh, L., Johansson, O., Sevger, P., McCarthy, T., &
593 Mishra, C. (2014). Vigorous dynamics underlie a stable population of the endangered
594 snow leopard panthera uncia in tost mountains, south gobi, mongolia. *PloS one*, *9*(7),
595 e101319.
- 596 Sharma, R. K., Bhatnagar, Y. V., & Mishra, C. (2015). Does livestock benefit or harm snow
597 leopards? *Biological Conservation*, *190*, 8–13.
- 598 Sollmann, R., Gardner, B., & Belant, J. L. (2012). How does spatial study design influence
599 density estimates from spatial capture-recapture models? *PloS one*, *7*(4), e34575.
- 600 Sun, C. C., Fuller, A. K., & Royle, J. A. (2014). Trap configuration and spacing influences
601 parameter estimates in spatial capture-recapture models. *PloS one*, *9*(2), e88025.

- 602 Sutherland, C., Fuller, A. K., & Royle, J. A. (2015). Modelling non-euclidean movement and
603 landscape connectivity in highly structured ecological networks. *Methods in Ecology and*
604 *Evolution*, 6(2), 169–177.
- 605 Wolters, M. A. (2015). A genetic algorithm for selection of fixed-size subsets with application
606 to design problems. *Journal of Statistical Software, Code Snippets*, 68(1), 1–18. doi:
607 10.18637/jss.v068.c01

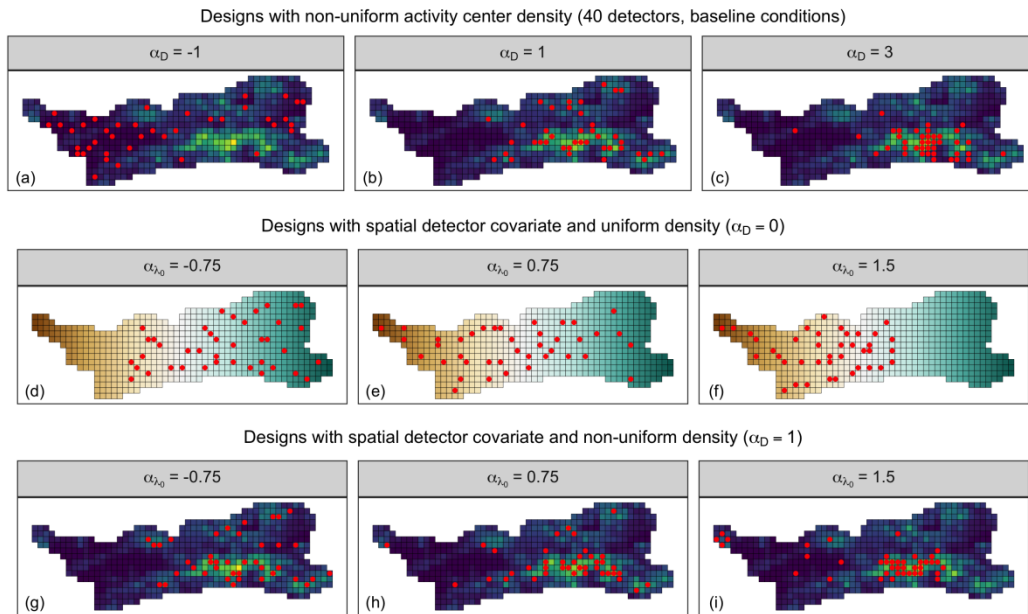




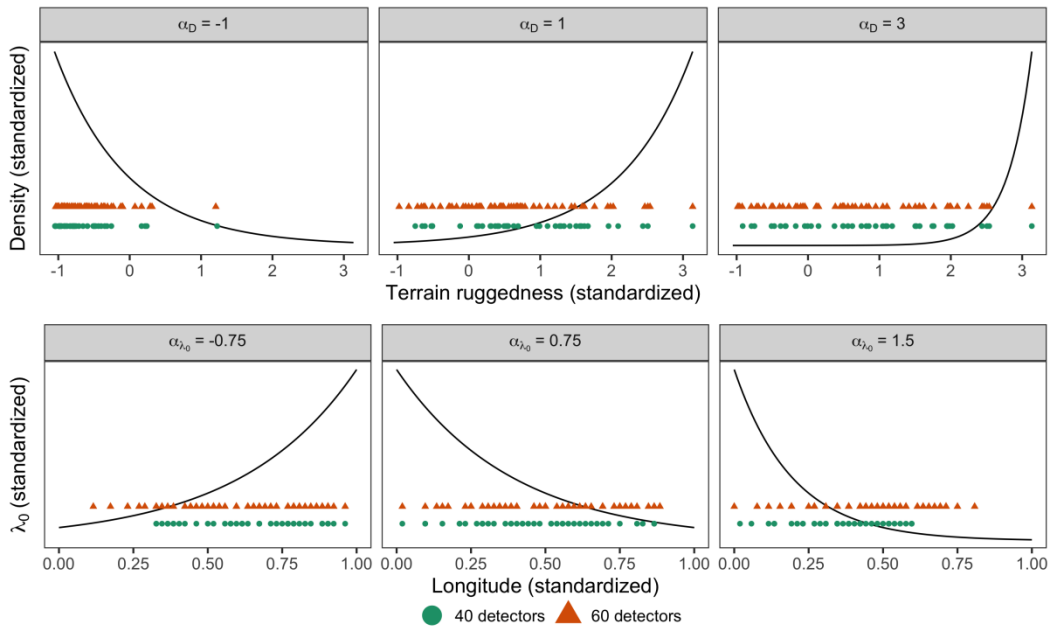
mee3_13517_f2.png



mee3_13517_f3.png



mee3_13517_f4.png



mee3_13517_f5.png